Nanoscale Res Lett (2009) 4:1103–1109
DOI 10.1007/s11671-009-9364-0

NANO EXPRESS

Synthesis of Tin Nitride Sn_xN_y Nanowires by Chemical Vapour Deposition

Matthew Zervos · Andreas Othonos

Received: 5 March 2009 / Accepted: 26 May 2009 / Published online: 20 June 2009

Abstract Tin nitride (Sn_xN_y) nanowires have been grown for the first time by chemical vapour deposition on n-type Si(111) and in particular by nitridation of Sn containing NH_4Cl at 450 °C under a steady flow of NH_3. The Sn_xN_y nanowires have an average diameter of 200 nm and lengths $\geq$5 μm and were grown on Si(111) coated with a few nm's of Au. Nitridation of Sn alone, under a flow of NH_3 is not effective and leads to the deposition of Sn droplets on the Au/Si(111) surface which impedes one-dimensional growth over a wide temperature range i.e. 300–800 °C. This was overcome by the addition of ammonium chloride (NH_4Cl) which undergoes sublimation at 338 °C thereby releasing NH_3 and HCl which act as dispersants thereby enhancing the vapour pressure of Sn and the one-dimensional growth of Sn_xN_y nanowires. In addition to the action of dispersion, Sn reacts with HCl giving $SnCl_2$ which in turn reacts with NH_3 leading to the formation of Sn_xN_y NWs. A first estimate of the band-gap of the Sn_xN_y nanowires grown on Si(111) was obtained from optical reflection measurements and found to be $\approx$2.6 eV. Finally, intricate assemblies of nanowires were also obtained at lower growth temperatures.

Keywords Tin nitride · Nanowires · Synthesis · Chemical vapor deposition

M. Zervos (✉)
Nanostructured Materials and Devices Laboratory,
Department of Mechanical and Manufacturing Engineering,
Materials Science Group, University of Cyprus,
P.O. Box 20537, 1678 Nicosia, Cyprus
e-mail: zervos@ucy.ac.cy

A. Othonos
Department of Physics, Research Centre of Ultrafast Science,
University of Cyprus, P.O. Box 20537, 1678 Nicosia, Cyprus

Introduction

Nitrides and in particular, group III-Nitride (III-N) compound semiconductors such as GaN, InN and AlN have been investigated intensively over the past decade due to their applications in electronic and optoelectronic devices like field effect transistors, light emitting diodes and lasers [1–3]. III-N semiconductors are especially attractive because their band-gap can be tailored from 0.7 eV in InN [4] up to 6.2 eV in AlN [5] but also due to the strained induced charges that provide an extra degree of freedom which can be used to tailor the band-profile and consequently the properties of devices [6].

However, in contrast to III-N compound semiconductors there are few investigations on group IV-Nitride (IV-N) compounds such as Ge_3N_4 [7, 8] and even less on Sn_3N_4 [9–22].

Tin nitride Sn_3N_4 is a relatively unknown semiconductor and the first investigation of Sn_3N_4 was carried out by F. Fisher et al. [9] as early as 1908. It has an energy band-gap that was estimated to be $\approx$1.5 eV [11] and so far Sn_3N_4 thin films have been grown by a variety of methods [12–19], including, atmospheric pressure chemical vapour deposition (APCVD) using halides [12, 13], metal organic chemical vapour deposition (MOCVD) [14], sputtering [15–18] and ammonothermal synthesis [19, 20]. Thin films of Sn_3N_4 have also been proposed as materials for optical storage [21, 22] since it was demonstrated that it dissociates into β-Sn upon exposure to a focused beam of light but also as a material for batteries [23].

Not surprisingly there are very few investigations on Sn_3N_4 nanostructured materials and it appears that the only study carried out so far concerns the synthesis of Sn_3N_4 nanoparticles (NPs) on Au coated Si(001) via chemical vapour deposition (CVD) using $SnCl_4 \cdot 5H_2O$ as a solid

precursor, by Nand et al. [24]. To date, there is no report on the synthesis of Sn_xN_y nanowires (NWs) despite the fact that nanowires constitute a fundamental building block for the development of nanoscale devices such as third generation solar cells which require low cost, nanostructured materials.

Therefore in order to complement our earlier investigations on the synthesis and properties of InN NWs and related oxides such as In_2O_3 and SnO_2 NWs [25–27], a preliminary investigation on the growth of Sn_xN_y NWs was undertaken.

Here the synthesis of the first Sn_xN_y NWs on Au/Si(111) is described and it is shown that Sn_xN_y nanowires (NWs) can not be grown via the direct nitridation of Sn over a broad range of temperatures i.e. between 300–800 °C due to the formation of Sn droplets on the surface of the Si(111). While there is evidence of one dimensional (1D) growth occurring at 500 °C via the direct nitridation of Sn, the yield is extremely poor. One-dimensional growth was promoted and significantly enhanced via the incorporation of NH_4Cl in the Sn and its sublimation which acts as a dispersant thereby enhancing the vapour pressure of Sn. Sn_xN_y NWs with an average diameter of 200 nm were obtained at 450 °C while intricate assemblies of NWs have also been obtained at lower temperatures.

Experimental Procedure

The Sn_xN_y NWs were grown using an APCVD reactor which consists of four mass flow controllers (MFC's) and a horizontal quartz tube furnace, capable of reaching a maximum temperature of 1,100 °C. Initially, fine Sn powder (Aldrich, < 150 μm, 99.5%) was loaded into a quartz boat together with a square piece of Si(111) approximately 7 mm × 7 mm in size, which was coated with a few nm's of Au. The Au layer was deposited via sputtering at a slow rate using an Ar plasma under a pressure $<10^{-4}$ mBar. The Au/Si(111) sample was positioned $\approx$ 5 mm downstream from the Sn and subsequently the boat was loaded into the APCVD reactor and positioned directly above the thermocouple used to measure the heater temperature at the centre of the quartz tube. After loading the boat at room temperature (RT), Ar (99.999%) was introduced at a flow rate of 500 standard cubic centimetres per minute (sccm) for 5 min in order to purge the tube and eliminate O_2 and H_2O. Following this the temperature was ramped to the desired growth temperature in a NH_3 flow of 250 sccm at a rate of 30 °C/min. Upon reaching the growth temperature (T_G) the flow of NH_3 was maintained at 250 sccm for a further 60 min after which the tube was allowed to cool down over at least an hour, in a flow of 50 sccm NH_3. The sample was removed only when the temperature was lower than 100 °C.

Table 1 Maximum diameter (Ø) of Sn droplets (DPs) and Sn_xN_y NWs obtained from heating up Sn under NH_3 and from the reaction of Sn + NH_4Cl respectively, at different temperatures. In all cases a ramp rate of 30 °C/min was used to reach T_G under 250 sccm's of NH_3 which was then maintained for a further 60 min at the growth temperature and after which the reactor was allowed to cool down to RT in a reduced flow of 50 sccm's NH_3

T_G (°C)	Max Ø of Sn DPs (Sn:NH_3)	Max Ø Sn_xN_y NWs (Sn + NH_4Cl:NH_3)
300	No DPs	No NWs
400	200 nm	200 nm
450	–	200 nm
500	500 nm	No NWs
600	500 nm	No NWs
700	2.0 μm	–
800	5.0 μm	–

In order to enhance the one dimensional growth of Sn_xN_y NWs an equal amount of anhydrous NH_4Cl (VWR Int 99.9%) was added to the Sn and mixed thoroughly in the boat. Then the same gas flows and temperature-time profile described above was employed. A summary of the temperatures and conditions is given in Table 1. The morphology of the Sn_xN_y NWs was examined with a TESCAN scanning electron microscope (SEM) while the crystal structure and the phase purity of the Sn_xN_y NWs were investigated using a SHIMADZU, XRD-6000, X-ray diffractometer with a Cu Ka source while a scan of θ–2θ in the range between 10° and 80° was performed. Finally optical spectroscopy was carried out using a standard spectrophotometer UV/V (Perkin–Elmer Lambda 950) in the reflection mode at near normal incidence to the surface of the sample.

Results and Discussion

As stated above the only investigation on the synthesis of nanostructured Sn_3N_4 is that of single phase, cubic tin nitride nanoparticles grown via atmospheric pressure-halide vapour phase epitaxy by Nand et al. [24]. In particular Nand et al. employed $SnCl_4 \cdot 5H_2O$ as a source of Sn and used 10 nm Au/Si(001) p-type substrates that were positioned at different distances from the $SnCl_4 \cdot 5H_2O$, along the reactor. The $SnCl_4 \cdot 5H_2O$ was heated up to 500 °C under a flow of NH_3 and N_2 and the temperatures of the samples along the reactor were 400, 300 and 150 °C, respectively. However, Nand et al. [21] did not obtain any NWs. Before discussing the synthesis of the Sn_xN_y NWs obtained here it is instructive to consider first the synthesis

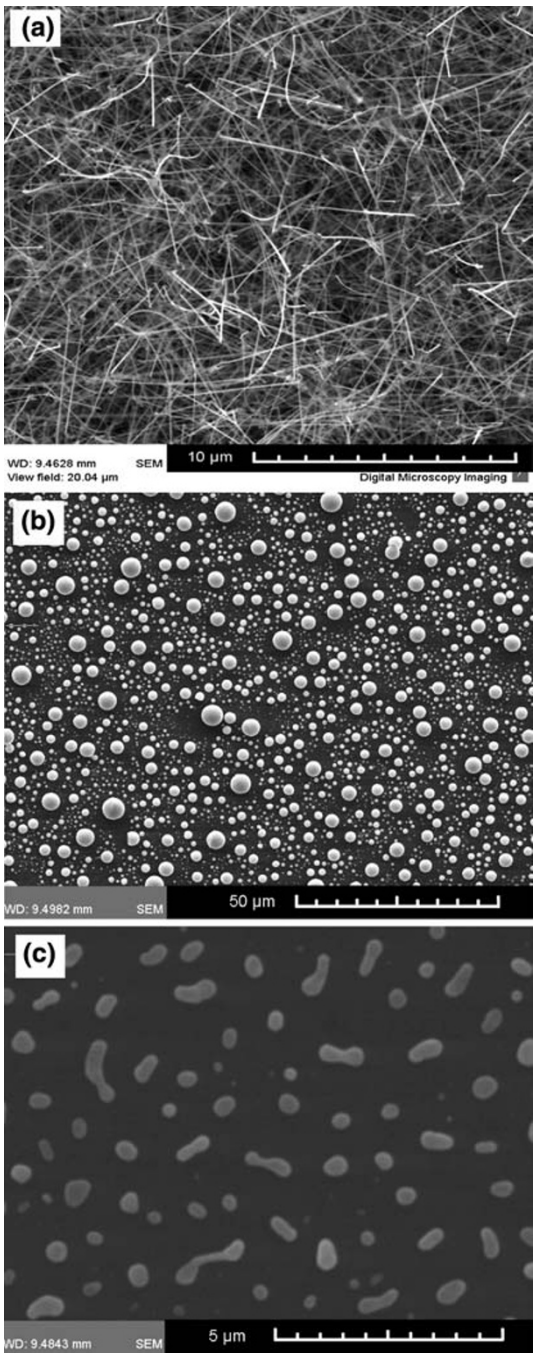

Fig. 1 SEM images of **a** SnO_2 NWs with an average diameter of 50 nm grown on Au/Si(111) at 800 °C in an inert gas flow of 100 sccm Ar. No droplets exist among the NWs **b** Sn droplets on Au/Si(111) deposited using the same temperature-time profile in **a** but in a steady gas flow of 250 sccm of NH_3 as opposed to Ar. A broad distribution in the sizes of the Sn droplets was obtained with diameters ≤5 μm **c** similar to **b** but smaller Sn droplets with diameters ≤0.5 μm were obtained at 500 °C many of which are also elongated

of SnO_2 NWs on 0.5 nm Au/Si(111) that were previously obtained by heating up Sn in an inert gas flow of 100 sccm Ar at 30 °C/min up to 800 °C and then maintaining the flow of Ar at this temperature for a further 90 min before cool down [27]. A typical SEM image of the SnO_2 NWs obtained in this way is shown in Fig. 1a from which it is clear that a large yield of SnO_2 NWs was obtained with an average diameter of 50 nm due to the reaction of Sn with residual O_2 in the APCVD reactor. Performing the reaction under a direct flow of O_2 leads to the formation of SnO_2 around the molten Sn which limits the vapour pressure significantly and hence the growth of NWs. As a consequence the molten Sn upstream always had a grey like, non reflective appearance at the end of the process, while no droplets were observed among the SnO_2 NWs. A similar process was also used recently for the growth of In_2O_3 NWs at 700 °C [26].

At first sight it would seem that the synthesis of Sn_xN_y NWs by direct nitridation of Sn with NH_3 is feasible by changing from Ar to NH_3 since Sn, like In, has a low melting point [28] and InN NWs have been obtained by direct nitridation of In with NH_3 at a heater temperature of 600 °C [25]. However, Sn_xN_y NWs were not obtained by the direct nitridation of Sn with NH_3. Instead many Sn droplets appeared on the Si(111) surface and a typical SEM image of such Sn droplets after the attempted nitridation of Sn with NH_3 at 800 °C is shown in Fig. 1b. The Sn droplets cover the entire surface and have a density of $\approx 10^7$ cm^{-2} and diameters ≤5 μm. Furthermore the size of the Sn droplets decreased as the temperature was reduced to 600 °C and many of then became elongated as shown in Fig. 1c.

The formation of large droplets on the Au/Si(111) surface during the direct nitridation of Sn with NH_3 is a direct consequence of the reducing action of NH_3 which eliminates the background O_2 in the APCVD reactor. This in turn prevents the formation of an oxide around the Sn and so the molten drop always had a highly reflective, metallic like surface. In contrast when Sn is heated up in a flow of pure, inert Ar, the surface is grey like and not reflective due to the O_2 background which is responsible for the formation of SnO_2 NWs that were grown optimally on 0.5 nm Au/Si(111) at 800 °C using the same temperature-time profile and Ar as opposed to NH_3 [27].

Apart from droplets, no nanostructures were obtained via the attempted nitridation of Sn with NH_3 in the temperature range 600 °C $< T_G <$ 800 °C. Turning on the flow of NH_3, after ramping up the temperature in an inert gas flow of Ar, did not lead to the growth of Sn_xN_y NWs either but again resulted into the deposition of Sn droplets. However, there was some evidence of one-dimensional growth at $T_G = 500$ °C. Literally a few NWs with diameters >500 nm's and lengths up to 3 μm appeared at a few locations on the Si(111) surface, hence the yield was extremely poor. Nevertheless, a further reduction of the growth temperature down to 300 °C did not lead to any

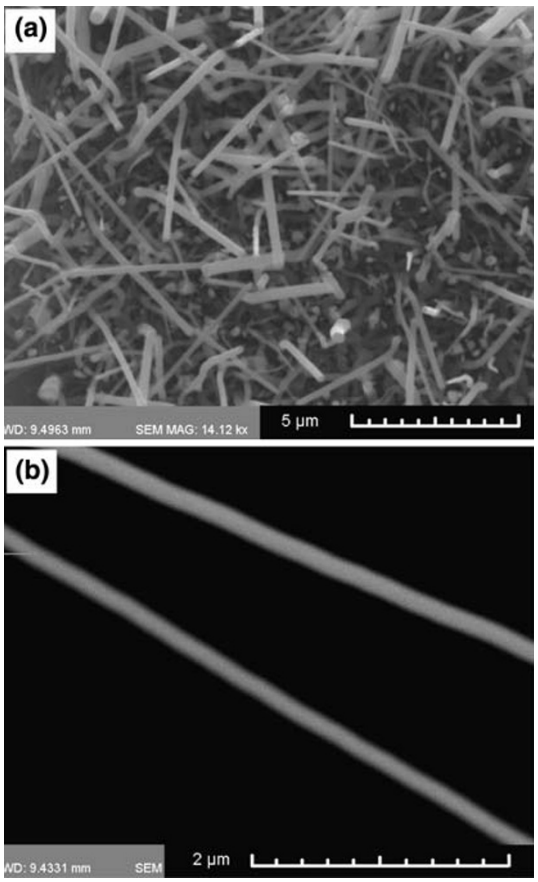

Fig. 2 **a** Sn_xN_y NWs grown on Au/Si(111) at the optimum temperature of 450 °C using a Sn:NH_4Cl mixture under a flow of 250 sccm's NH_3 **b** high magnification SEM image of Sn_xN_y NWs

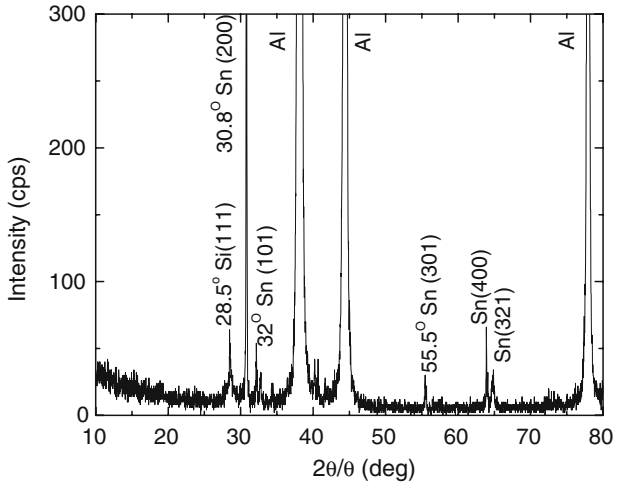

Fig. 3 XRD spectrum of Sn droplets deposited on Si(111) at 800 °C under a flow of 250 sccm NH_3

significant deposition on the Si, no NWs were obtained and moreover, the Sn upstream lost its metallic shine due to the build up of a black deposit on the molten Sn which limited the vapour transport. In addition, no differences were observed upon changing the flow rate of NH_3 during the growth while keeping everything else equal at all temperatures so the direct nitridation of Sn alone under a flow of NH_3 is not effective and leads to the deposition of Sn droplets on the Au/Si(111) surface which impedes one-dimensional growth over a wide temperature range i.e. 300–800 °C as shown below in Table 1.

The XRD spectrum of the Sn droplets deposited at 800 °C is shown in Fig. 3 and is characterized by an intense peak corresponding to the (2 0 0) orientation of Sn and less intense but well resolved peaks corresponding to the (1 0 1), (3 0 1), (4 0 0) and (3 2 1) orientations. In addition to the Sn droplets the Al holder peaks have also been identified but no peaks associated with Sn_xN_y were found.

These findings are in direct contrast with the case of InN where NWs can be grown by direct nitridation of In with NH_3 via a self-catalytic mechanism. The optimum heater temperature for the growth of InN NWs was found to be 600 °C where its vapour pressure is equal to 10^{-6} Torr. Large In droplets comparable in size to those in Fig 1b started appearing only at temperatures $\geq$800 °C in contrast to the Sn droplets whose density was large and persisted even down to 600 °C where its vapour pressure is $<10^{-11}$ Torr. It appears therefore that the Sn droplets are born out from the melt upstream and are transferred to the Si(111) surface where they coalesce to form larger droplets.

The tendency for one-dimensional growth observed at $T_G = 500$ °C during the direct nitridation of Sn with NH_3 was promoted by the addition of NH_4Cl into the Sn at a ratio of 1:1 by weight. The reaction of NH_4Cl with Sn was carried out under a flow of NH_3 keeping the flow rate, ramp rate and temperature profile identical to those used in the case of 'direct nitridation' of Sn with NH_3. A typical SEM image of Sn_xN_y NWs obtained by the reaction of Sn with NH_4Cl under NH_3 at 450 °C is shown in Fig 2a. The Sn_xN_y NWs have an average diameter of 200 nm's and lengths up to 5 μm while the reaction of Sn with NH_4Cl always lead to the deposition of a white powder downstream, near the cool end of the reactor, in contrast to the direct nitridation of Sn with NH_3 where no by products occurred.

The XRD spectrum of the Sn_xN_y NWs grown at 450 °C is shown in Fig. 4 and is characterized by the (2 2 0), (3 1 1), (5 1 1) and (4 4 0) peaks, which can be indexed to the hexagonal structure of Sn_3N_4 [18]. The intense peak of Sn(200) observed in Fig. 3 has disappeared and once more the Al peaks appearing in the XRD spectrum of Fig. 4 due to the sample holder have been identified. Furthermore there are no peaks associated with SnO_2 [27].

The promotion of one dimensional growth is attributed to the dissociation of NH_4Cl. Upon increasing the temperature NH_4Cl undergoes sublimation at 338 °C and

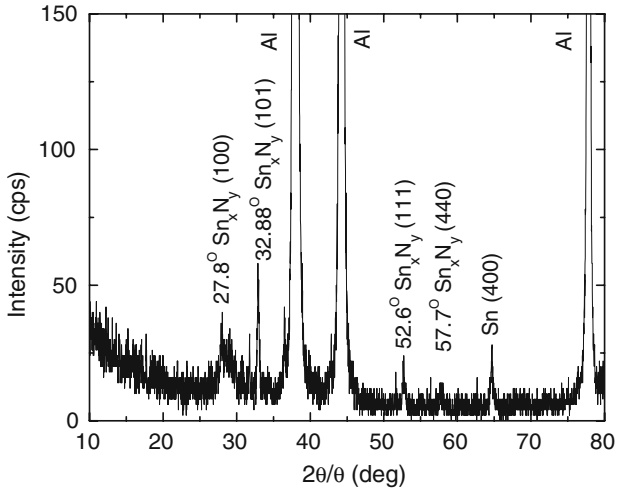

Fig. 4 XRD spectrum of Sn_xN_y NWs grown on Au/Si(111) at 450 °C via the reaction of Sn and NH_4Cl

therefore dissociates into NH_3 and HCl according to the following reaction.

$$NH_4Cl_{(S)} \rightarrow NH_3 + HCl \quad (1)$$

As explained by Chaiken et al. [29] the sublimation rate of NH_4Cl increases by a factor of 10^4 when changing the temperature from $T = 100$ to 600 °C and the typical sublimation weight loss of NH_4Cl is over 90% when heated for ≈60 min. It is interesting to point out here that this sublimation process is endothermic and the temperature is expected to be reduced only by a few tens °C in the case of NH_4Cl [29]. The decomposition of NH_4Cl enhances the porosity of the Sn melt and more importantly acts as a dispersant increasing the amount of Sn that is transferred into the gas stream. In fact the sublimation of NH_4Cl and the generation of NH_3 and HCl gasses which act to disperse the molten Sn occurs abruptly and leads to strong dispersion of the molten Sn inside the boat for the ramp rate used here i.e. 30 °C/min suggesting that lower ramp rates would be more suitable. In addition to acting as a dispersant, the sublimation of NH_4Cl yields HCl which reacts with Sn leading to the formation of $SnCl_2$ according to the reaction,

$$Sn + 2HCl \rightarrow SnCl_2 + H_2 \quad (2)$$

Note that $SnCl_2$ melts at 38 °C and decomposes above 600 °C. Subsequently the $SnCl_2$ reacts with NH_3 according to,

$$3SnCl_2 + 4NH_3 \rightarrow Sn_3N_4 + 6HCl + 6H_2 \quad (3)$$

Consequently the role of the NH_4Cl is two fold. First, it prevents the Sn from melting up into one single drop and second it supplies the necessary HCl for the formation of $SnCl_2$. As stated above heating up Sn alone in NH_3 did not lead to the deposition of any products near the cool end of the reactor so the deposition that occurs from heating up Sn and NH_4Cl in NH_3 is due to the reaction of Sn with HCl since XRD of the deposit showed no peaks related to NH_4Cl.

The reaction outlined above is in a way similar to that put forward by Nand et al. [21] whereby $SnCl_4$ reacts with NH_3 according to,

$$3SnCl_4 + 4NH_3 \rightarrow Sn_3N_4 + 12HCl \quad (4)$$

leading to the growth of Sn_3N_4 NPs on 10 nmAu/Si(111) that were placed at various positions along the reactor but also similar to the growth of Sn_3N_4 thin films by APCVD using halides, by Gordon et al. and Takahashi et al. [12, 13].

A similar kind of reaction was also used to grow InN nanocrystals on Si(111) whereby the incorporation of NH_4Cl into the In lead to the complete elimination and transfer of the In into the gas stream where it formed primarily InCl which in turn reacted with the NH_3 leading to the formation of InN nanocrystals with diameters of 300 nm [30].

While the addition of NH_4Cl in Sn did not result into its complete transfer in the gas stream like with In, it provided nonetheless the necessary HCl for the formation of $SnCl_2$ which subsequently reacts with NH_3 on the Au/Si(111) leading to the one dimensional growth of Sn_xN_y. Interestingly the distance of the sample from the Sn:NH_4Cl mixture was found to be critical and for distances >10 mm the reaction led to the formation of closely packed NPs with sizes <100 nm on the Au/Si(111) most probably due to the lower vapour pressure of the $SnCl_2$.

Although the details of the growth mechanism are not understood thoroughly at present it is suggested that the Sn_xN_y NWs grow self catalytically from Sn_xN_y NPs although the role of the Au which appears to enhance the one dimensional growth still needs to be clarified [32, 33].

A first estimate of the band-gap of the Sn_xN_y nanowires grown on Si(111) was obtained from optical reflection measurements using a UV–IR spectrometer at near normal incidence on both the NW sample and the Si(111) substrate for comparison, shown in Fig. 5. Clearly evident is the distinct difference in the reflection spectra from the substrate and the NWs. Also evident is the band edge of the Sn_xN_y NWs which is estimated to be approximately 2.6 eV [31].

In addition to Sn_xN_y NWs that were obtained at $T_G = 450$ °C there is also evidence for the formation of more complex nanostructures obtained for $T_G < 450$ °C as shown in Fig. 6a and b. However, their density was smaller compared to that in Fig. 2a due to the lower growth temperature which limits the amount of Sn transferred over to the Si(111). The radial growth of NWs from the droplet shown in Fig 6a is very similar to the case of InN [25] whereby nucleation centres form on the surface of droplets which then facilitate radial growth [32]. Moreover, the circular arrangement of NWs shown in Fig. 6b is due to

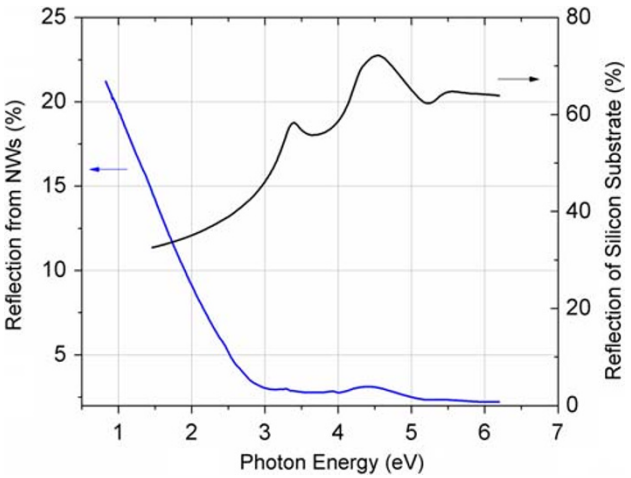

Fig. 5 Optical reflection from the Sn_xN_y NWs (*Left*) and plain *n*-type Si(111) substrate (*Right*)

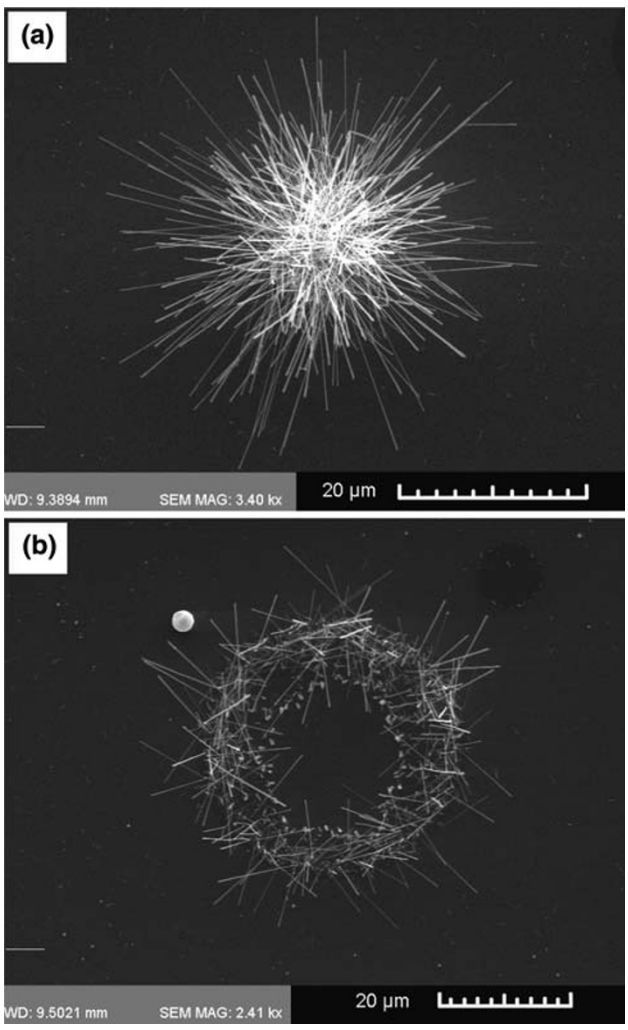

Fig. 6 Nanostructures obtained at $T = 400$ °C on 0.7 nm Au/Si(111) **a** NWs emanating from a droplet and **b** NWs which have grown from droplets in a circular configuration

the formation of droplets that accumulate near the periphery of well defined circles similar to the growth of In_2O_3 nano pyramids that self assemble in the form of wreaths due to the reaction of In with NH_4Cl in a flow of N_2 [30].

Conclusions

The first tin nitride, Sn_xN_y nanowires have been grown by CVD on Au coated Si(111) via the reaction of Sn with NH_4Cl at 450 °C under a steady flow of NH_3. Attempting direct nitridation of Sn with NH_3 leads to the formation of Sn droplets due to the reducing action of the NH_3 which eliminates O_2 in the reactor and which in turn inhibits one-dimensional growth over a wide temperature range between 300–800 °C. The formation of large Sn droplets was suppressed by adding NH_4Cl which dissociates into NH_3 and HCl by sublimation at 338 °C and acts as a dispersant thereby enhancing the vapour pressure of Sn. Furthermore the Sn reacts with HCl and yields $SnCl_2$ which subsequently reacts with NH_3 leading to the formation of Sn_xN_y nanowires which have diameters of 200 nm and lengths up to 5 µm. Finally nanowires protruding from droplets and intricate assemblies of NWs arranged in the shape of wreaths were also obtained at temperatures <450 °C. The synthesis of metal (M)-nitride i.e. M_xN_y nanowires where the metal component is readily available and has a low cost, is expected to be important for third generation solar cells based on nanostructured semiconductor materials.

Acknowledgments The work in this article was supported by the *Research Promotion Foundation of Cyprus* (www.research.org.cy) under grant BE0308/03 for fundamental research in the area of nanotechnology and nanomaterials.

References

1. S. Seo, G.Y. Zhao, D. Pavlidis, Electron. Lett. **44**, 244 (2008)
2. Y. Taniyasu, M. Kasu, T. Makimoto, Nature **441**, 325 (2006)
3. S. Nakamura, T. Mukai, M. Sengh, Appl. Phys. Lett. **64**, 1687 (1994)
4. J. Wu, W. Walukiewicz, K.M. Yu, J.W. Ager, E.E. Haller, H. Lu, W.J. Schaff, Y. Saito, Y. Nanishi, Appl. Phys. Lett. **80**, 3967 (2002)
5. J. Li, K.B. Nam, M.L. Nakarmi, J.Y. Lin, H.X. Jiang, P. Carrier, Su.-Huai. Wei, Appl. Phys. Lett. **83**, 5163 (2003)
6. M. Zervos, A. Kostopoulos, G. Constantinidis, M. Kayambaki, A. Georgakilas, J. Appl. Phys. **91**, 4387 (2001)
7. M. Yang, S.J. Wang, Y.P. Feng, G.W. Peng, Y.Y. Sun, J. Appl. Phys. **102**, 013507 (2007)
8. T. Maeda, T. Yasuda, M. Nishizawa, N. Miyata, Y. Morita, S. Takagi, J. Appl. Phys. **100**, 014101 (2006)
9. F. Fisher, G. Iliovichi, Ber., Deut. Chem. Ges. **41**, 3802 (1908)
10. F. Fisher, G. Iliovichi, Ber., Deut. Chem. Ges. **42**, 527 (1909)

11. T. Lindgren, M. Larsson, S.-E. Lindquist, Proc. 14th Int. Workshop on Quantum Solar Energy Conversion, 2002
12. R.G. Gordon, D.M. Hoffman, U. Riaz, Chem. Mater. **4**, 4 (1992)
13. N. Takahashi, K. Terada, T. Nakamura, J. Mat. Sci. Lett. **20**, 227 (2001)
14. D.M. Hoffman, S.P. Rangarajan, S.D. Athavale, D.J. Economou, J.-R. Liu, Z. Zheng, W.-K. Chu, J. Vac. Sci. Technol. A. **13**, 820 (1995)
15. Y. Inoue, M. Nomiya, O. Takai, Vacuum **51**, 673 (1998)
16. R. Kamei, T. Migita, T. Tanaka, K. Kawabata, Vacuum **59**, 764 (2000)
17. L. Maya, J. Vac. Sci. Technol. A. **11**, 604 (1993)
18. R.S. Lima, P.H. Dionisio, W.H. Schreiner, Solid State Commun. **79**, 395 (1991)
19. B. Wang, M.J. Callahan, Cryst. Growth Des. **6**, 1227 (2006)
20. L. Maya, Inorg. Chem. **31**, 1958 (1992)
21. N. Takahashi, M. Takekawa, T. Takahashi, T. Nakamura, M. Yoshioka, Y. Kawata, Solid State Sci. **5**, 587 (2003)
22. T. Maruyama, T. Morishita, Appl. Phys. Lett. **69**, 890 (1996)
23. K.S. Park, Y.J. Park, M.K. Kim, J.T. Son, H.G. Kim, S.J. Kim, J. Pow. Sour. **103**, 67 (2001)
24. S.V. Nand, K. Ankur, K. Brijesh, M.B. Raj, Solid State Sci. **10**, 569 (2008)
25. A. Othonos, M. Zervos, M. Pervolaraki, Nanoscale Res. Lett. **4**, 122–129 (2009)
26. D. Tsokkou, A. Othonos, M. Zervos, Ultrafast time resolved spectroscopy of In_2O_3 nanowires, Nanotechnology, (2009) (In Press)
27. A. Othonos, M. Zervos, D. Tsokkou, Nanoscale Res. Lett. (2009) DOI 10.1007/s11671-009-9323-9
28. In melts at 156.61 °C while Sn melts at 231.93°C
29. R.F. Chaiken, D.J. Sibbett, J. Sutherland, D.K. Van de Mark, A. Wheeler, J. Chem. Phys. **37**, 2311 (1962)
30. M. Zervos, D. Tsokkou, M. Pervolaraki, A. Othonos, Nanoscale Res. Lett. (2009). DOI 10.1007/s11671-009-9266-1
31. Vipin. Kumar, Sachin. Kr. Sharma, T.P. Sharma, V. Singh, Opt. Mater. **12**, 115 (1999)
32. Z. Zhang, J. Gao, L.M. Wong, J.G. Tao, L. Liao, Z. Zheng, G.Z. Xing, H.Y. Peng, T. Yu, Z.X. Shen, C.H.A. Huan, S.J. Wang, T. Wu, Nanotechnology **20**, 135605 (2009)
33. H.J. Fan, A.S. Barnard, M. Zacharias, Appl. Phys. Lett. **90**, 143116 (2007)